

FE PREDICTION OF BEARING CAPACITY FACTOR OF SHALLOW FOUNDATION UNDER THREE-DIMENSIONAL STRAIN CONDITION

Nilthson N. Valverd^a, Christianne L. Nogueira^b and Celso Romanel^a

^a*Programa de Pós-Graduação em Engenharia Civil, Departamento de Engenharia Civil, Pontifícia Universidade Católica do Rio de Janeiro, Rua Marquês de São Vicente, 225, Gávea, Rio de Janeiro/RJ, Brasil, CEP 22453-900, nilthson@aluno.puc-rio.br, romanel@puc-rio.br.*

^b*Programa de Pós-Graduação em Engenharia Mineral, Universidade Federal de Ouro Preto, Departamento de Engenharia de Minas, Campus Universitário Morro do Cruzeiro, Ouro Preto/MG, Brasil – CEP 35400-000, chris@em.ufop.br*

Keywords: *ultimate bearing capacity, bearing capacity factor, shallow foundation, three dimensional analysis, finite elements methods, Modified Mohr-Coulomb model.*

Abstract. This paper presents a numerical model for three dimensional elastoplastic analysis of bearing capacity problems in shallow foundation using a displacement formulation of the finite element method (FEM). The non-linear equation solution strategies and the stress integration algorithm are presented and discussed. The soil foundation is modeled as a non-associative elastoplastic Mohr-Coulomb material. The ultimate bearing capacity factor obtained numerically for various friction and dilatancy angles is compared to solutions by using limit equilibrium, limit analysis, and other three dimensional FEM analyses. Good agreement is observed between them. A parametric study is conducted in order to verify the influence foundation roughness on the ultimate bearing capacity. The results show that there is no significant difference in the ultimate bearing capacity factor.

1 INTRODUCTION

An application of the finite element method (FEM) for non-linear elastoplastic analysis of shallow foundation under three-dimensional strain condition is presented in this paper.

The Modified Mohr-Coulomb criterion suggested by Sloan & Booker (1986) and Abbo & Sloan (1995), which includes treatment of the singularities of the original Mohr-Coulomb criterion, is used for modeling the foundation soil. A general formulation that considers associative and non-associative elastoplastic models for soil was adopted and used to investigate the influence of the dilatancy angle on the bearing capacity of the shallow foundation.

A parametric study considering different friction and dilatancy angles, shape and roughness of footing, and loading condition (displacement or force control) was conducted using the code ANLOG – *Non Linear Analysis of Geotechnical Problems* (Zornberg 1989; Nogueira 1998; Oliveira 2006, Nogueira et al 2007, Nogueira et al 2008).

2 FINITE ELEMENT EQUATIONS

In considering an incremental formulation using FEM, the algebraic equation system that represents the static equilibrium for the soil represented by its elemental volume dV_e can be written as:

$$\Delta \mathbf{F}_{int} = \Delta \mathbf{F}_{ext} \quad (1)$$

where $\Delta \mathbf{F}_{ext}$ represents the external force increment and,

$$\Delta \mathbf{F}_{int} = \int_{V_e} \mathbf{B}^T \Delta \boldsymbol{\sigma} dV_e \quad (2)$$

represents the internal force incremental of internal force. \mathbf{B} is a kinematic operator that describes the relationship between the strain increment ($\Delta \boldsymbol{\epsilon}$) and the nodal displacement increment ($\Delta \hat{\mathbf{u}}$) in each element.

$$\Delta \boldsymbol{\epsilon} = -\mathbf{B} \Delta \hat{\mathbf{u}} \quad (3)$$

The operator \mathbf{B} depends on the type of element adopted. The negative sign in Eq. (3) is a conventional indicator of positive compression. The stress increment ($\Delta \boldsymbol{\sigma}$) is obtained using the incremental constitutive equation:

$$\Delta \boldsymbol{\sigma} = \mathbf{D}_t \Delta \boldsymbol{\epsilon} \quad (4)$$

where \mathbf{D}_t is the constitutive matrix defined in terms of the elastoplasticity formulation as:

$$\mathbf{D}_t = \mathbf{D}_e - \mathbf{D}_p \quad (5)$$

where \mathbf{D}_e is the elastic matrix and \mathbf{D}_p is the plastic parcel of the constitutive matrix defined as:

$$\mathbf{D}_p = \frac{\mathbf{D}_e \mathbf{b} (\mathbf{D}_e \mathbf{a})^T}{\mathbf{a}^T \mathbf{D}_e \mathbf{b} + H} \quad (6)$$

In which, H is the hardening modulus, \mathbf{a} is the gradient of the yield function ($F(\boldsymbol{\sigma}, h)$) and \mathbf{b} is the gradient of the potential plastic function ($G(\boldsymbol{\sigma}, h)$), where h is the hardening parameter. In the case of perfect plasticity, where hardening is not considered, $F = F(\boldsymbol{\sigma})$, $G = G(\boldsymbol{\sigma})$ and H equals zero.

Starting from an equilibrium configuration (Figure 1) where the displacement field and the strain and stress states are all known, a new equilibrium configuration, in terms of displacements, can be obtained using the modified Newton Raphson procedure with automatic load increment (Nogueira 1998). For a selected tolerance, and at each increment, the iterative scheme satisfies the global equilibrium, compatibility conditions, boundary conditions and constitutive relationships. Yet attention must be given to the stress integration scheme adopted to obtain the stress increments, Eq. (4), in order to guarantee the Kuhn-Tucker conditions and the consistency condition. Figure 1 illustrates the described process.

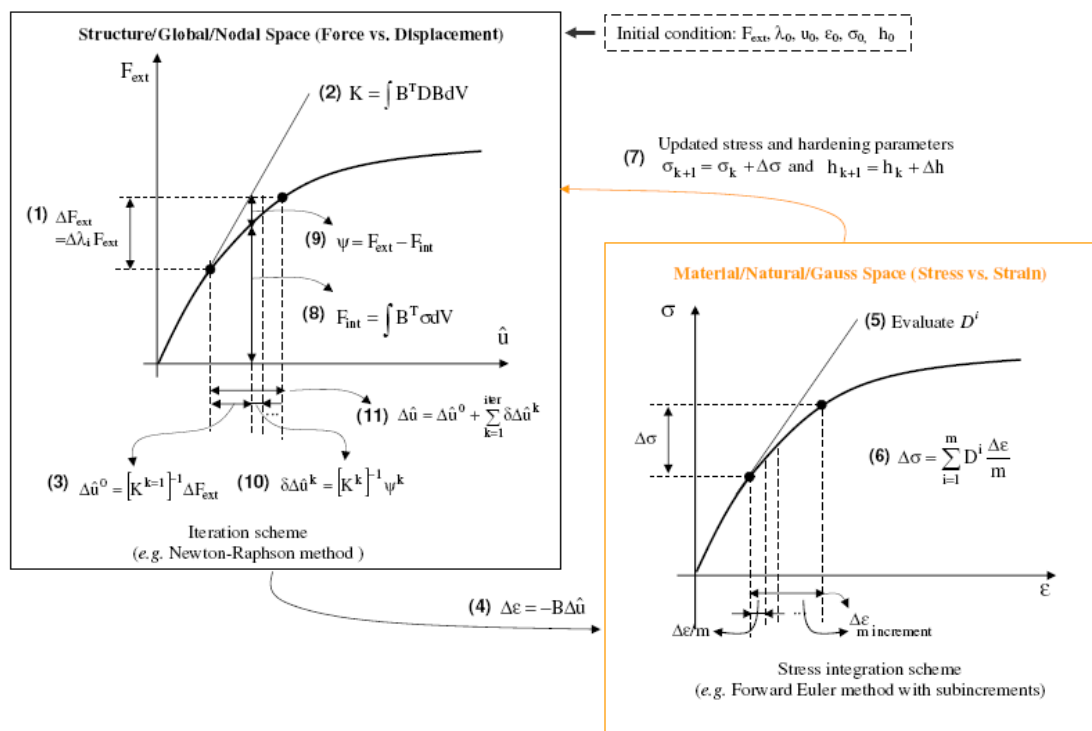


Figure 1: Scheme for solving the non linear equilibrium equation (Yang 2009)

The finite element adopted in this study is the quadratic cubic isoparametric element (C20). This element has three degrees of freedom, u , v and w , in the x , y and z directions, respectively. The stress and strain vectors are defined as:

$$\boldsymbol{\sigma}^T = [\sigma_x \quad \sigma_y \quad \sigma_z \quad \tau_{xy} \quad \tau_{yz} \quad \tau_{zx}] \quad (7)$$

$$\boldsymbol{\epsilon}^T = [\epsilon_x \quad \epsilon_y \quad \epsilon_z \quad \gamma_{xy} \quad \gamma_{yz} \quad \gamma_{zx}] \quad (8)$$

The kinematic operator \mathbf{B} can be written as:

$$\mathbf{B}_i = \nabla N_i = \begin{bmatrix} \partial N_i / \partial x & 0 & 0 & \partial N_{20} / \partial x & 0 & 0 \\ 0 & \partial N_i / \partial y & 0 & 0 & \partial N_{20} / \partial y & 0 \\ 0 & 0 & \partial N_i / \partial z & \dots & 0 & 0 & \partial N_{20} / \partial z \\ \partial N_i / \partial y & \partial N_i / \partial x & 0 & \dots & \partial N_{20} / \partial y & \partial N_{20} / \partial x & 0 \\ 0 & \partial N_i / \partial z & \partial N_i / \partial y & & 0 & \partial N_{20} / \partial z & \partial N_{20} / \partial y \\ \partial N_i / \partial z & 0 & \partial N_i / \partial x & & \partial N_{20} / \partial z & 0 & \partial N_{20} / \partial x \end{bmatrix} \quad (9)$$

where N_i is the i node shape function by the finite element C20 (Bathe 1982).

To describe the stress-strain relationship, a perfectly elastoplastic model with non-associative plasticity was adopted. The plastic parcel of the constitutive matrix is obtained using the modified Mohr-Coulomb criterion proposed by Sloan & Booker (1986) and Abbo & Sloan (1995) (Figure 2). The modified version of the Mohr-Coulomb model involves removal of the singularities at the edges ($\theta = \pm \pi/6$) and the apex of the original model. Its yield function is written as:

$$F = \sqrt{I_{2D}(K(\theta))^2 + (a \sin \phi)^2} - (I_1/3) \sin \phi - c \cos \phi \quad (10)$$

where

$$\theta = (1/3) \sin^{-1} \left((-1.5\sqrt{3}) I_{3D} (I_{2D})^{-3/2} \right) \quad \theta \in [-\pi/6; \pi/6] \quad (11)$$

I_1 is the first invariant of the stress tensor I_{2D} is the second invariant of the deviator stress tensor, I_{3D} is the third invariant of the deviator stress tensor, c and ϕ are the material cohesion and internal friction angle, respectively. A transition angle (θ_T) was introduced to define the $K(\theta)$ function for Eq. (10). Sloan & Booker (1986) suggest a θ_T value range from 25° to 29°. For the case in which $|\theta| > \theta_T$,

$$K(\theta) = A + B \sin 3\theta \quad (12)$$

where

$$A = (1/3) \cos \theta_T \left(3 + \tan \theta_T \tan 3\theta_T + (1/\sqrt{3}) \text{signa}(\theta) (3 \tan \theta_T - \tan 3\theta_T) \sin \phi \right) \quad (13)$$

And

$$B = (1/(3 \cos 3\theta_T)) \left(-\text{signa}(\theta) \sin \theta_T + (1/\sqrt{3}) \cos \theta_T \sin \phi \right) \quad (14)$$

Or, for the case in which $|\theta| \leq \theta_T$

$$K(\theta) = \cos \theta + (1/\sqrt{3}) \sin \theta \sin \phi \quad (15)$$

The parcel $a \sin \phi$ was introduced to prevent the singularity related to the surface apex. The potential plastic function (G) can be written the same way as the yield function (F) but using the dilatancy angle (ψ) instead of the friction angle (ϕ).

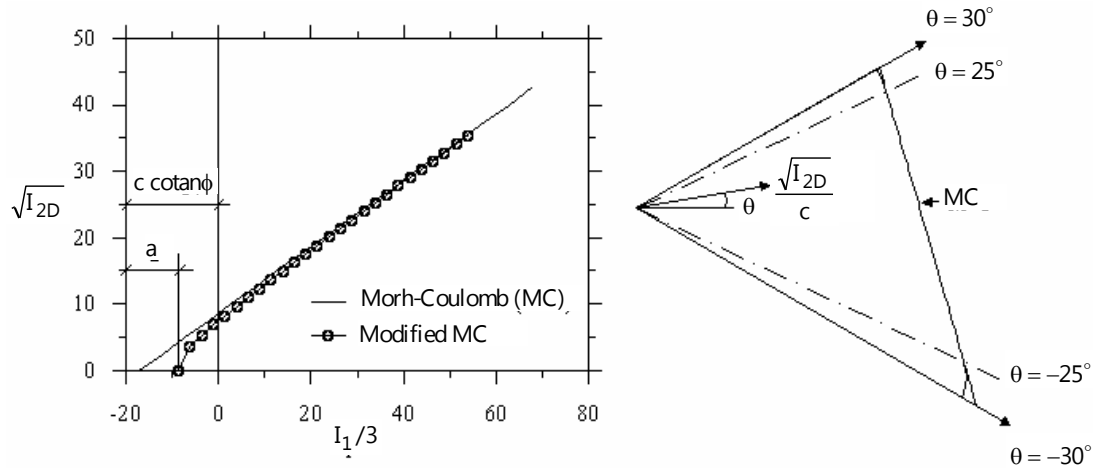


Figure 2: Mohr-Coulomb yield function (Adapted from Abbo & Sloan 1995)

An important step in a non linear analysis using FEM relates to the integration of the constitutive equation. This equation defines a set of ordinary differential equations for which the integration methodology can be either implicit or explicit. In this paper an explicit process with sub increments, as proposed by Sloan et al. (2001), was adopted. This methodology uses the modified Euler scheme that determines the size of the sub increment automatically evaluating the local error induced during integration of the parcel stress plasticity (Oliveira 2006).

Starting from an equilibrium configuration where the stress and strain states (σ_n and ϵ_n) are known, the elastic predict stress state can be evaluated doing:

$$\sigma_{n+1}^* = \sigma_n + \Delta\sigma \tag{16}$$

The stress increment $\Delta\sigma$ in Eq. (15) is evaluated using the elastic constitutive matrix as the tangent constitutive matrix. The yield function is evaluated for this new trial stress state and if $F(\sigma_{n+1}^*) \leq 0$, then an elastic response is observed and the strain increment $\Delta\epsilon$ generates just elastic stress increment. However, if $F(\sigma_{n+1}^*) > 0$, there will be a plastic flux and the increment of stress must be reevaluated. In this case, three possibilities can occur (Figure 3):

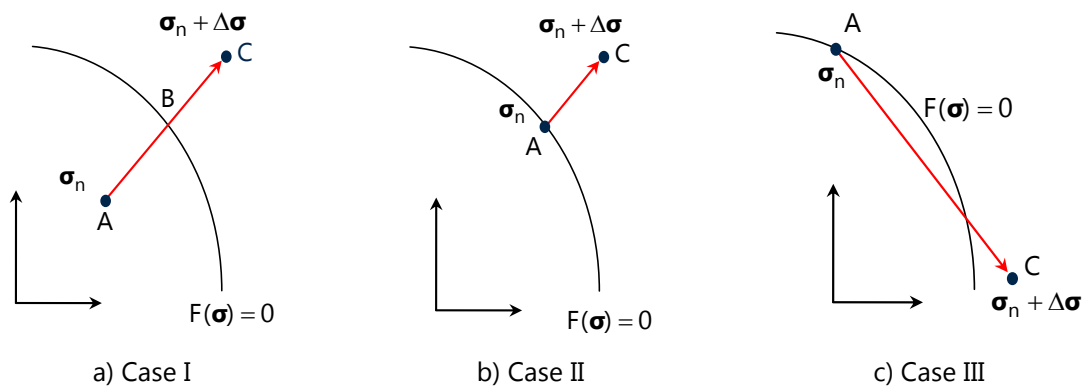


Figura 3: Trial stress state (Oliveira 2006)

Case I – the stress state was initially elastic and during the deformation path, the stress state changes from elastic to plastic, that is, $F(\sigma_n) < 0$ and $F(\sigma_{n+1}^*) > 0$.

Case II - the stress state was initially plastic and during the deformation path, the stress state remains plastic, that is $F(\sigma_n) = 0$ and $F(\sigma_{n+1}^*) > 0$.

Case III - the stress state was initially plastic and the deformation path includes an elastic unloading followed by a plastic loading.

Because of arithmetic precision, an approximated condition is used to verify the yield condition, that is

$$|F(\sigma_{n+1}^*)| \leq FTOL \quad (17)$$

where $FTOL$ is a small positive tolerance which Sloan et al. (2001) has suggested be no higher than 10^{-6} and no lower than 10^{-9} . With this approximation, the elastic to plastic transition will occur if $F(\sigma_n) < -FTOL$ and $F(\sigma_{n+1}^*) > FTOL$.

In Cases I and III, the strain increment has two parcels: elastic and plastic, that need to be determined since Euler's modified integration process will be applied just to the plastic parcel of the strain. So to obtain the elastic parcel of strain to integrate it in the strain increment, the following equation must be evaluated:

$$F(\sigma_n + \alpha \Delta \sigma) = 0 \quad (18)$$

where α is a scalar that varies between 0 to 1. If α is equal to zero, the strain increment is completely plastic (Case II) and if α is equal to 1, the strain increment is completely elastic (Case I). Case III occurs when the angle between σ_n and $\Delta \sigma$ is higher than 90° and $F(\sigma_{n+1}^*) > FTOL$.

After solving the Eq. (18) the elastic and plastic parcels of the strain increment are obtained doing:

$$\Delta \epsilon_e = \alpha \Delta \epsilon, \quad (19)$$

$$\Delta \epsilon_p = (1 - \alpha) \Delta \epsilon. \quad (20)$$

And the stress limit at the yield surface that defines the elastic region (σ_{int}) is so obtained by doing:

$$\sigma_{int} = \sigma_n + D_e \Delta \epsilon_e. \quad (21)$$

The integration process begins from the σ_{int} stress state, dividing the plastic parcel of strain increment, Eq. (20), into k sub-increments with $\Delta T_k(1-\alpha)\Delta \epsilon$ magnitudes, where ΔT_k depends on the error committed during the stress evaluation.

To each strain sub-increment the integration process starts calculating two approximation values for the stress increments:

$$\Delta \sigma_1 = D_t(\sigma_{k-1})[\Delta T_k(1-\alpha)\Delta \epsilon], \quad (22)$$

$$\Delta \sigma_2 = D_t(\tilde{\sigma}_k)[\Delta T_k(1-\alpha)\Delta \epsilon]. \quad (23)$$

For the first sub-increment ($T=0$), the first estimation of the stress increment $\Delta \sigma_1$ is evaluated considering the limit stress, $\sigma_{k-1} = \sigma_{int}$, and for the second estimation, the stress increment is evaluated considering the stress state at the end of the first estimation $\tilde{\sigma}_k = \sigma_{k-1} + \Delta \sigma_1$ (Euler scheme). The stress state σ_k at the end k^{th} sub-increment is obtained according to the modified Euler scheme as:

$$\sigma_k = \sigma_{k-1} + \frac{1}{2}(\Delta \sigma_1 + \Delta \sigma_2) \quad (24)$$

The local error committed can be defined as the difference between the stress states obtained by the Euler scheme ($\tilde{\sigma}_k$) and the stress states obtained by the modified Euler scheme (σ_k) that is:

$$\sigma_k - \tilde{\sigma}_k = \frac{1}{2}(\Delta \sigma_2 - \Delta \sigma_1) \quad (25)$$

Sloan et al. (2001) has suggested the following expression for the relative error for the current sub-increment:

$$R_k = \|\sigma_k - \tilde{\sigma}_k\| / \|\sigma_k\| \quad (26)$$

This current sub-increment would be accepted, if the relative error R_k is lower than the tolerance $STOL$, otherwise the process will restart by assigning another value to the sub-increment ΔT_k evaluated, taking into consideration the local error and the tolerance adopted as:

$$\Delta T_{k+1} = q \Delta T_k \quad (27)$$

In which,

$$q \leq 0.9 \sqrt{STOL / R_k} \quad (28)$$

This integration process automatically controls the number of sub-increments in terms of the magnitude of the plastic deformation and the adopted tolerance $STOL$.

3 SHALLOW FOUNDATION ANALYSES IN 3D STRAIN CONDITION

The analyses presented in this study involve a smooth and rough, flexible and rigid square footing foundation (2B width) subjected to vertical loading acting on the ground surface. The problem is analyzed under three dimensional strain conditions (taking into account the geometric symmetry) and is modeled as both a flexible and rigid foundation using load and displacement controls respectively (Figure 4). The rough foundation was modeled prescribing null horizontal displacement for the nodal points on the surface beneath the foundation while they were made free for smooth foundation. The foundation soil is considered weightless.

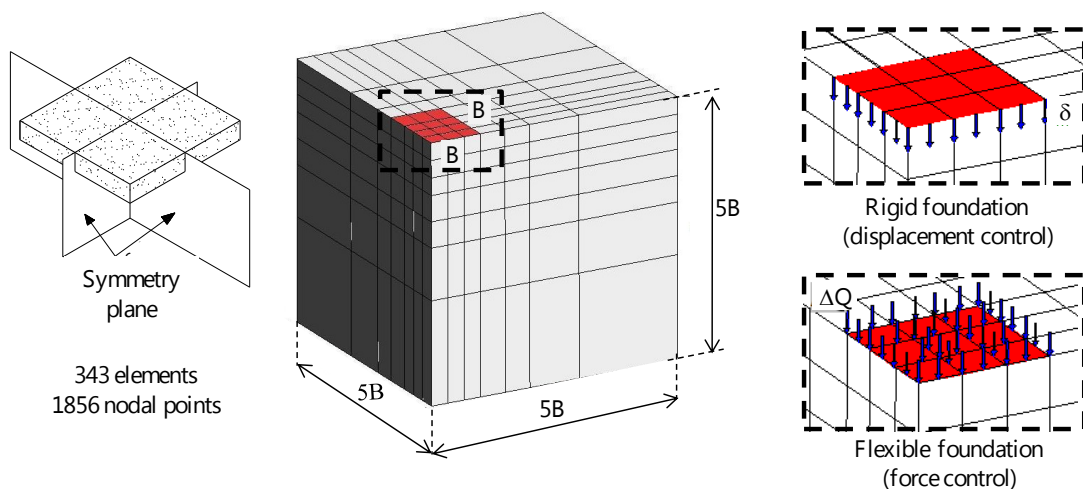


Figure 4: 3D analyses of shallow foundation – fem mesh for smooth and rough, flexible and rigid square footing.

As mentioned, the soil is considered as an elastic perfectly plastic material described by a non-associative modified Mohr-Coulomb model. The following parameters were adopted: $E=100\text{MPa}$; $\nu=0.30$; $c=10\text{kPa}$; $a=15\%$; $\theta_r=28^\circ$. Both the friction and dilatancy angle were varied to assess their influence on the bearing capacity factor of the shallow foundation.

The tolerance used at global level during the Newton-Raphson iterative process was 10^{-4} while the tolerance used at Gauss level during the stress integration scheme was $STOL$ of 10^{-6} and $FTOL$ of 10^{-6} .

Numerical results are presented in terms of the κ factor which is a normalized stress defined as:

$$\kappa = (Q/A)/c = q/c \quad (29)$$

in which Q is the reaction force at the foundation, defined as:

$$Q = \sum_{e=1}^n \left(\int_{V_e} \mathbf{B}^T \boldsymbol{\sigma}_e dV_e \right) \quad (30)$$

The reaction force is evaluated as the sum of the internal force's vertical components equivalent to the elements' stress state (σ_e) right beneath the foundation. The cohesion is adopted to normalize the results. For pure frictional soil, the atmospheric pressure of 1atm substitutes the cohesion in Eq. (29).

Figure 5 presents the κ factor versus normalized settlement (δ/B) curves obtained by ANLOG for flexible and rigid smooth foundations and for different values of friction and dilatancy angles.

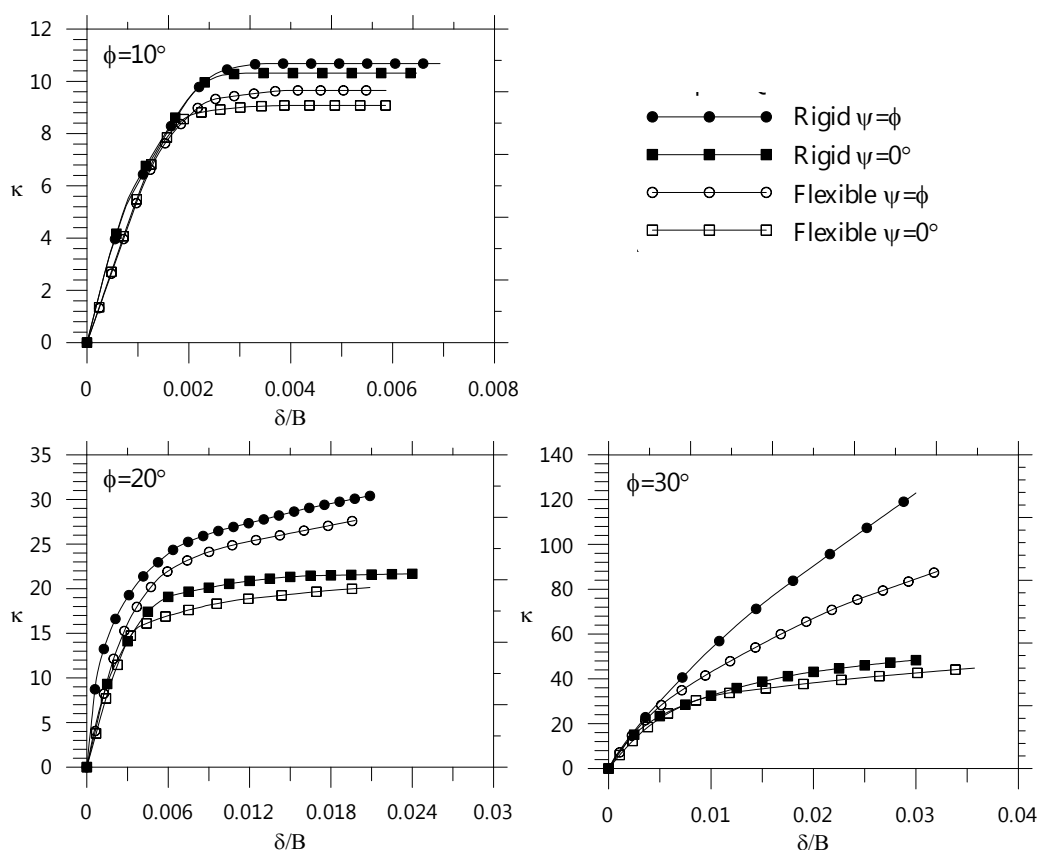


Figure 5: Normalized load-displacement curves – smooth shallow foundation.

The bearing capacity of the shallow foundation is related to the ultimate bearing capacity factor (κ_{ult}) which has been differently defined by several authors. Trautmann and Kulhawy (1988) adopted the tangent method that defines κ_{ult} as the κ factor at the intersection point between the elastic and plastic tangents of the normalized load-displacement curve. Briaud and Jean (1994) suggested as κ_{ult} the κ factor for a normalized displacement of 10%. Table 1 shows the ultimate bearing capacity factor obtained in this study considering the tangent method.

Houlsby (1991) presented a study about the influence of dilatancy on soil behavior. He concluded that dilatancy plays an important role in geotechnical problems where the soil has movement restrictions, such as shallow foundations, slope stability and tunnels.

$\phi(^{\circ})$	$\psi(^{\circ})$	smooth	rough
------------------	------------------	--------	-------

		flexible	rigid	flexible	rigid
10	0	9.08	10.31	5.82	6.91
	10	9.65	10.67	5.87	7.32
20	0	20.13	21.92	16.10	16.70
	20	22.84	23.85	16.90	21.5
30	0	44.83	48.60	20.20	21.30
	30	49.68	51.30	22.30	23.60

Table1: Ultimate bearing capacity factor κ_{ult} for flexible and rigid, rough and smooth shallow foundation.

Analyses conducted in this study show that when the friction angle was decreased to 10° , the ultimate bearing capacity factor was slightly affected by the dilatancy angle. For a friction angle of 30° , the associate plasticity analysis ($\psi=\phi$) provided the highest ultimate bearing capacity factor and the lowest displacement at failure. Zienkiewicz et al. (1975) observed a similar response for friction angles of 40° . Monahan & Dasgupta (1995) reported such behavior for friction angles higher than 25° .

As expected, the κ_{ult} value obtained for a rigid foundation is higher than that obtained for a flexible foundation. The difference in normalized ultimate bearing capacity values was approximately 10% for both non-associate and associate plasticity; independently of its roughness.

Table 2 presents a comparison between results obtained using ANLOG (by considering a rigid, smooth foundation and associate plasticity) and those from a classical solution from equilibrium limit by Terzaghi (1943), limit analyses solution by Chen (1975), and others 3D analysis using FEM by Michalowski (2001) and Yang et al (2003).

$\phi=\psi(^{\circ})$	This study	Terzaghi (1943)	Chen (1975)	Michalowski (2001)	Yang et al (2003)
10	10.67	10.86	9.98	12.66	9.77
20	23.85	19.29	20.10	31.84	19.47
30	51.3	39.18	49.30	104.01	42.07

Table2: Ultimate bearing capacity factor κ_{ult} for rigid smooth square footing.

Good agreement is observed between the results provided by this study and Terzaghi (1943). Nevertheless, the equilibrium limit theory underestimates the ultimate bearing capacity factor for highest friction angle. Results differ from each author due to the method used to define the ultimate bearing capacity factor; but in general, they show good agreement.

In order to verify the influence of the foundation size, a parametric study was conducted by varying the L/B ratio (length/width) of a smooth and rigid foundation.

Figure 6 shows the FEM mesh used and the normalized load-displacement curve for different L/B ratios. The tangent of the normalized load-displacement becomes steeper as the L/B ratio decreases. For L/B ratio equal to 5, the ultimate bearing capacity factor reaches 35.63 (Table 3), which is very close to 32.4 value obtained by Oliveira (2006) for a rigid smooth strip footing foundation. So the plane strain condition can be observed for an L/B ratio higher than 5.

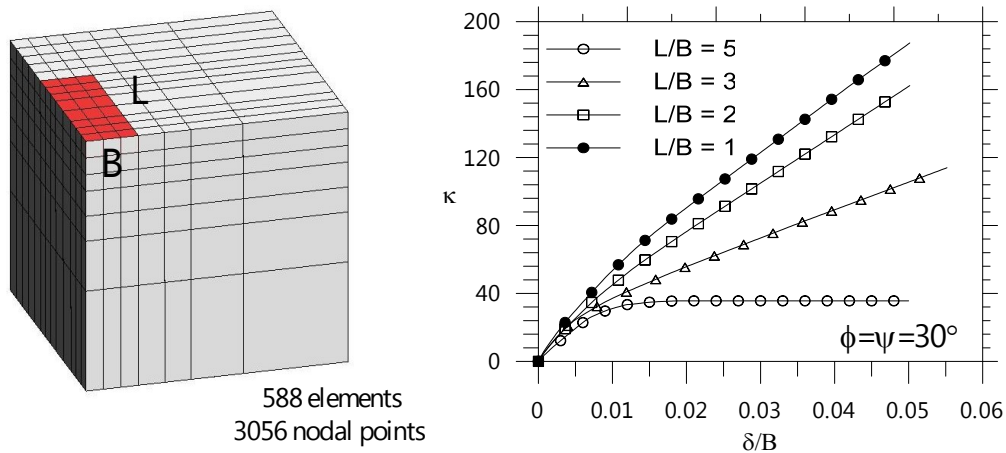


Figure 6: Normalized load-displacement curves L/B=variable.

L/B	1	2	3	5
κ_{ult}	51.30	44.60	39.10	35.63

Table3: Ultimate bearing capacity factor κ_{ult} - smooth rigid foundation - L/B=variable.

An undrained analysis was conducted considering the same FEM mesh presented in Figure 4 and adopting $\phi=0^\circ$; $\nu=0.49$ and $S_u=100\text{kPa}$. Figure 7 shows the normalized load-displacement curves for smooth and rough, rigid and flexible foundations. As expected, the κ_{ult} value obtained for a rigid and rough foundation is higher than that obtained for a flexible and smooth foundation.

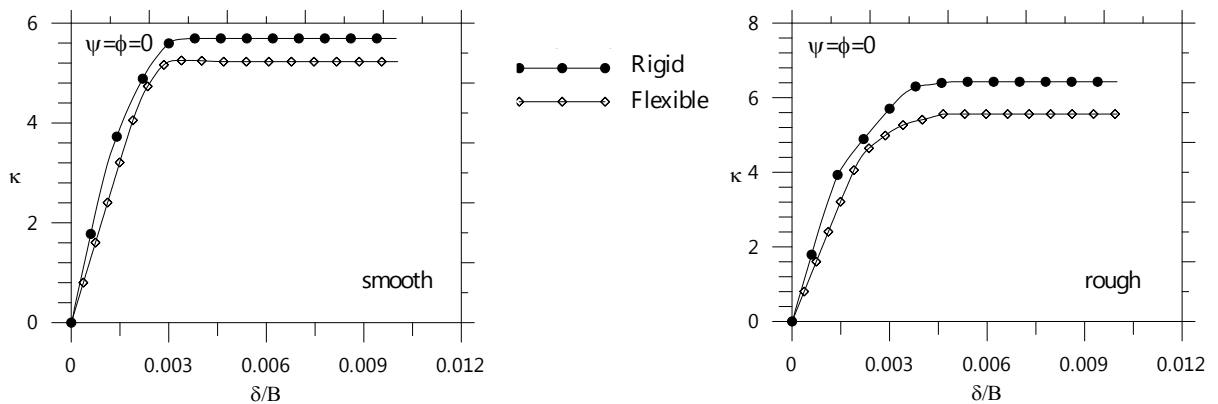


Figure 7: Normalized load-displacement curves – undrained analysis.

Table 4 shows the ultimate bearing capacity factor obtained in this study and by Potts and Zdravkovic (2001), Yang et al (2003) and Michalowski (2001). Good agreement is observed between them.

foundation		This study	Potts e Zdravkovic (2001)	Yang et al (2003)	Michalowski (2001)
rigid	smooth	5.69	5.72	-	-
	rough	6.42	6.37	6.174	6.830

Table3: Ultimate bearing capacity factor κ_{ult} - undrained analysis.

4 CONCLUSIONS

This paper presented a numerical simulation using FEM to analyze the bearing capacity of shallow foundations under three dimensional conditions. The implementation of the explicit integration stress algorithm proposed by Sloan et al (2001) was needed in order to obtain good performance of the Newton Raphson algorithm at the global level.

The numerical results confirmed that the ultimate bearing capacity factor of a rigid and rough shallow foundation is higher than that on a flexible and smooth shallow foundation. The ultimate bearing capacity factor of rigid foundations obtained numerically shows good agreement with the results obtained by equilibrium limit theory (Terzaghi 1943), limit analysis (Chen 1975) and others 3D FEM analyses (Potts and Zdravkovic 2001, Yang et al 2003 and Michalowski 2001).

The ultimate bearing capacity factor was slightly affected by the dilatancy angle when the friction angle is low but was highly affected for comparatively high friction angles. Therefore, for a high friction angle the normalized ultimate bearing capacity factor values are a little high in the case of associative plasticity. In general, the non-associative plasticity provides higher settlement at failure. Results presented in this paper agree with the results provided by Monahan & Dasgupta (1995) and Zienkiewics et al (1975).

The plane strain condition is a particular one verified for L/B ratio higher than 5.

ACKNOWLEDGMENTS

The authors are grateful for the financial supports received from PROCAD - CAPES (National Academic Cooperation Program - Coordinating Agency for Advanced Training of High-Level Personnel – Brazil). They also acknowledge Harriet Reis for the editorial review of this text.

REFERENCES

- Abbo, A.J. and Sloan, S.W., A smooth hyperbolic approximation to the Mohr-Coulomb yield criterion. *Computers & Structures*, 54(3): 427-441, 1995.
- Bathe, K. J., *Finite Element Procedures in Engineering Analysis*. Prentice-Hall v1, 1982.
- Briaud, J.L. and Jeanjean, P., Load Settlement Curve Method for Spread Footings on Sand. *Vertical and Horizontal Deformations of Foundations and Embankments*, ASCE. Vol. 2, pp. 1774-1804, 1994.
- Chen, W.F., *Limit Analysis and Soil Plasticity*. Elsevier Science Publishers, BV, Amsterdam, Netherlands, 1975.
- Houlsby, G.T., How the dilatancy of soils affects their behavior. *In: Proc. X Euro. Conf. Soil Mech. Found. Engng.*, Firenze 1991, (4):1189-1202, 1991.
- Manohan, N. and Dasgupta, S.P., Bearing capacity of surface footings by finite element. *Computers & Structures*, (4): 563-586, 1995.
- Michalowski, R.L., Upper bound load estimates on square and rectangular footings. *Geotechnique* 51 (9), 787, 2001.
- Nogueira, C. L.; Oliveira, R. R.V and Zornberg, J. G., FE Prediction of Bearing Capacity of Reinforced Soil under Plane Strain Condition. *In: First Pan American Geosynthetics Conference and Exhibition - Geoamérica*, Cancun. Mexico. R.J. Bathurst & E.M.palmeira, 2008. v.1. p.1 – 10, 2008
- Nogueira, C.L., Non-linear analysis of excavation and fill. *DSc. Thesis*. PUC/Rio, RJ, 265p (*in Portuguese*), 1998.
- Nogueira, C.L.; Oliveira, R.R.V.; Araújo, L.G.; Faria, P.O. and Zornberg, J.G., FE prediction of bearing capacity over reinforced soil - *5th International Workshop on Applications of Computational Mechanics in Geotechnical Engineering*, Guimarães, Portugal, 1-4 April, 2007.
- Oliveira, R.R.V., Elastoplastic analysis of reinforced soil structures by FEM. *MSc. Thesis*. PROPEC/UFOP (*in Portuguese*), 2006
- Potts, D. M. and Zdravković, L, *Finite Element Analysis in Geotechnical Engineering: Application*, vol.2, Thomas Telford, 2001
- Sloan, S.W. and Booker, J.R., Removal of singularities in Tresca and Mohr-Coulomb yield criteria, *Communications in Applied Numerical Methods*, (2): 173-179, 1986.
- Sloan, S.W.; Abbo, A.J. and Sheng, D., Refined explicit integration of elastoplastic models with automatic error control, *Engineering Computations*, 18(1): 121-154, 2001.
- Terzaghi, K., *Theoretical Soil Mechanics*, Wiley, 1943.
- Trautmann, C.H. and Kulhawy, F.H., Uplift Load-Displacement Behavior of Spread Foundations. *Journal of Geotechnical Engineering*, ASCE, Vol. 114, No. 2, pp. 168-183, 1988.
- Yang, H., Shen, Z. and Wang, J., 3D lower bound bearing capacity of smooth rectangular surface footings. *Mechanics Research Communications* 30 (2003) 481-492, 2003

- Yang, KH, Stress distribution within Geosynthetic-Reinforced Soil Structures. *PhD. Dissertation* – Depart. of Civil Engineering - University of Texas at Austin, 2009.
- Zienkiewicz, O.C., Humpheson, C. and Lewis, R.W., Associated and non-associated visco-plasticity and plasticity in soil mechanics. *Geotechnique*, 25(4): 671-689, 1975.
- Zornberg, J.G., Finite element analysis of excavations using an elasto-plastic model. *MSc. Thesis*. PUC-Rio, Rio de Janeiro (*in Portuguese*), 1989.